Belgian Institute for Space Aeronomy
(BIRA-IASB)

SACS+

Extension of the "Support to Aviation Control Service"

Algorithm Theoretical Basis Document

ESRIN/RFQ/3-12596/09/I-EC

December 2010

Table of Contents

1 Introduction

1.1 Scope of this document

In this document, an introduction is given to the basics of retrieval of volcanic SO2 and aerosol data using satellite nadir spectral measurements in the UV and infrared. The algorithms are implemented for use in near real time as part of the project SACS+ (extension of the "Support to Aviation Control Service").

1.2 The SACS project

The SACS (Support to Aviation Control Service) project is an ESA funded project aiming to deliver data in near-real time from measurements by space-based instruments regarding sulphur dioxide (SO_2) and aersol emissions possibly related to volcanic eruptions. This is achieved using polar-orbiting satellite instruments, measuring in the UV-visible (SCIAMACHY, OMI and GOME-2) and the infrared (IASI). SACS primary objective is to support the Key Users of the service (the Volcanic Ash Advisory Centres -VAACs) by sending an alert by email in case of exceptional concentrations of SO2 detected. The User is then redirected to a single user-friendly web portal (http://sacs.aeronomie.be) centralizing maps, data (including archive) and useful information.
The SACS team consists of three institutes: BIRA-IASB, KNMI and ULB.

1.3 Acronyms and abbreviations

AAI	Absorbing Aerosol Index
AMF	Air Mass Factor
ASCII	American Standard Code for Information Interchange
ASTER	Advanced Spaceborne Thermal Emission and Reflection Radiometer
ATBD	Algorithm Theoretical Basis Document
BIRA-IASB	Belgian Institute for Space Aeronomy
BTD	Brightness Temperature Difference
CCD	Charge-Couple Device
CEOS	Committee on Earth Observation Satellites
CMA	Center of Mass Altitude
DOAS	Differential Optical Absorption Spectrometry
DLR	German Aerospace Center
DU	Dobson Unit
DUE	Data User Element
ECMWF	European Centre for Medium-Range Weather Forecasts
ENVISAT	ENVIronmental SATellite
EOS	Earth Observation System
EPP	Equator Passing Point
ESA	European Space Agency

ESRIN	European Space Agency Research Institute
EUMETSAT	EUropean organization for the exploitation of METeorological SATellites
FRESCO	Fast Retrieval Scheme for Cloud Observables
GOME-2	Global Ozone Monitoring Instrument (aboard MetOp)
HDF	Hierarchical Data Format
IASI	Infrared Atmospheric Sounding Interferometer (aboard MetOp)
IAVW	International Airways Volcano Watch
ICAO	International Civil Aviation Organization
IR	Infrared
KMI-IRM	Royal Meteorological Institute of Belgium
KNMI	Royal Netherlands Meteorological Institute
LF	Linear Fit
LIDORT	Linearized Discrete Ordinate RTM
LUT	Look-Up-Table
MetOp-A	Meteorological Operational satellite-A
N/A	Not Applicable
NASA	National Aeronautics and Space Administration
NRT	NRT
O3MSAF	Ozone Monitoring Satellite Application Facility
OMI	Ozone Monitoring Instrument
PBL	Planetary Boundary Layer
PVD	Product Validation Document
RCP	Radiative Cloud Pressure
RTM	Radiative Transfer Model
SACS	Support to Aviation Control Service
SAVAA	Support to Aviation for Volcanic Ash Avoidance
SCD	Slant Column Density
SCIAMACHY	SCanning Imaging Absorption spectroMeter for Atmospheric CartograpHY (aboard ENVISAT)
SPSD	Service Portfolio Specification Document
STL	STratospheric Low
SO2	Sulfur Dioxide
SZA	Solar Zenith Angle
TBD	To Be Defined / Described
TOA	Top Of the Atmosphere
TOMS	Total Ozone Mapping Spectrometer
TRL	TRoposhere Low
TRM	TRoposhere Middle
UK	United Kingdom
ULB	Université Libre de Bruxelles
US	United States
UTC	Universal Time Coordinated
UV-VIS	Ultraviolet-Visible
VAAC	Volcanic Ash Advisory Centre

VCD	Vertical Column Density
VZA	Viewing Zenith Angle

1.4 Applicable documents

[AD1] ESA/ESRIN Statement of Work, ref. CEOS-INPR-EOPG-SW-09-0001, issued February 2009, of ESRIN/RFQ/3-12596/09/I-EC, Issue 1 rev 1.

[AD2] SACS+: Extension of the "Support to Aviation Control Service" in Support of the CEOS Atmospheric Composition Constellation, I: Technical Proposal, issued June 2009.

[AD3] SACS+: Extension of the "Support to Aviation Control Service" in Support of the CEOS Atmospheric Composition Constellation, I: Management Proposal, issued June 2009.

2 Satellite instruments

2.1 SCIAMACHY

The Scanning Imaging Absorption Spectrometer for Atmospheric CHartographY instrument (SCIAMACHY) is in operation on the ENVISAT platform since July 2002. In the nadir and limb viewing geometries, the SCIAMACHY instrument measures the sunlight scattered by the Earth's atmosphere or reflected by the surface whereas in the occultation mode, the direct solar or lunar light transmitted through the atmosphere is observed. The measurements are performed in eight spectral channels covering the 240-2400 nm wavelength range with a spectral resolution of 0.2 to 1.5 nm. A detailed description of the instrument and its characteristics can be found in Bovensmann et al. (1999).
The instrument fly on polar sun-synchronous orbits and it crosses the equator at 10:00h local time (descending node). In its nadir view, the SCIAMACHY swath width is of 960 km with pixels of 60x30 km². As a consequence of the alternating nadir and limb views, global coverage is only achieved in six days.

2.2 OMI

The Dutch-Finnish Ozone Monitoring Instrument (OMI) is a nadir-looking imaging spectrograph measuring direct and atmosphere backsctared sun radiation in the UV-visible range from 270 to 500 nm with a spectral resolution of ~0.6 nm. A description of the instrument and its characteristics are given in Levelt et al. (2006).
OMI is onboard the NASA's EOS Aura satellite on a polar sun-synchronous polar orbit with local equator crossing time at 13:40 local time. In its nominal mode, OMI has a spatial resolution of 13x24 km². The field of view of OMI corresponds to a 2600 km wide spatial swath, leading to complete global coverage in one day. It should be stressed that due to a row on the CCD detectors, the level1 radiance data of OMI are altered at all wavelengths for a particular viewing direction of OMI. This row anomaly (changing over time) can affect the quality of the products and hence reduce the spatial coverage of the data.

2.3 GOME-2

The second Global Ozone Monitoring Experiment (GOME-2) is a UV/visible spectrometer covering the 240-790 nm wavelength interval with a spectral resolution of 0.2 – 0.5 nm (Munro et al., 2006). GOME-2 measures the solar radiation backscattered by the atmosphere and reflected from the surface of the Earth in a nadir viewing geometry. A solar spectrum is also measured via a diffuser plate once per day. The ground pixel size is 80 x 40 km² and the full width of a normal GOME-2 scanning swath is 1920 km. Global coverage is achieved within 1.5-3 days at the equator and within one day poleward of ± 45°. The GOME-2 instrument was launched on board the Meteorological Operational satellite-A (MetOp-A) in October 2006. The MetOp-A satellite is in a sun-synchronous polar orbit with an equator crossing time of 09:30 local time on the descending mode.

The main objective of GOME-2 is the global monitoring of the total ozone field. However, the good spectral resolution and coverage of the instrument also allows for the retrieval of a number of other absorbing trace gases such as NO_2, SO_2, H_2CO, CHOCHO, OClO, H_2O and BrO, as well as cloud and aerosol parameters.

2.4 IASI

The Infrared Atmospheric Sounding Interferometer (IASI) is a Fourier transform spectrometer on board MetOp-A, measuring the spectrum emitted by the Earth and atmosphere in the thermal infrared spectral range, using nadir geometry. The spectral range coverage is from 645 cm^{-1} to 2760 cm^{-1} with a resolution of 0.5 cm^{-1} and a spectral sampling of 0.25 cm^{-1}. It provides global coverage twice a day with a footprint of 12 km diameter and full swath width of 2200 km. The equator crossing time is at about 09:30 local time in the morning and 21:30 in the evening. A description of the IASI instrument can be found in Clerbaux et al. (2009).

3 Sulphur dioxide algorithms

3.1 SO2 column retrieval from UV-visible observations: SCIAMACHY, OMI and GOME-2

Satellite UV-visible instruments, such as SCIAMACHY, OMI and GOME-2, measure the intensity of the sunlight in a nadir-viewing geometry, as function of the wavelength. The measured earthshine spectra accounts for all photons reaching the instruments that have been scattered by air molecules, aerosols and clouds or reflected by the surface of the Earth. This is depicted in Figure 1.

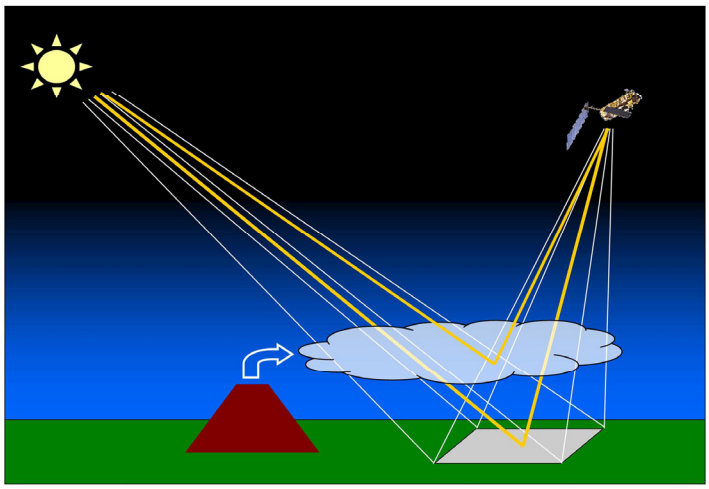

Figure 1: Sketch of a nadir-viewing satellite UV-visible measurement.

Along the different light paths, some of the photons are absorbed by the trace gases in the atmosphere (e.g., SO_2). Therefore the ratio between the measured earthshine spectra and the solar (absorption free) spectrum provides information on the amount of these absorbing trace gases in the atmosphere. However, it contains the signal from all species absorbing along the mean light path.
The SO_2 vertical columns are retrieved from the observations of the satellite instruments listed above (see examples in Figure 2) using the well-known DOAS (Differential Optical Absorption Spectroscopy) approach which consists in three main steps:

1. The atmospheric absorbers (in particular SO_2) are separated using the characteristic differential structures of their absorption cross-sections.The retrieved quantity can be interpreted as the integrated SO_2 concentration along the mean slant light path, it is the so-called slant column density (SCD). The spectral evaluation consists in a least-squares fit procedure where atmospheric cross-sections are adjusted to the log-ratio of a measured and a reference spectrum in a selected wavelength interval. The residual broadband features due to Rayleigh and Mie scattering are removed using a low-pass fitering method.

2. A background correction is applied to the retrieved SO_2 SCDs in order to avoid non-zero columns over regions known to have very low SO_2 and to insure a geophysical consistency of the results at high solar zenith angles.
3. The corrected SO_2 slant column is converted into a SO_2 vertical column (VCD). This implies the calculation of an air mass factor (AMF=SCD/VCD) which characterize the enhancement of the light path w.r.t. the vertical path. The AMF computation is done using simulations of the transfer of the radiation in the atmosphere. It requires accounting for parameters influencing the photons path (and hence the measurement sensitivity): solar zenith angle, instrument viewing angles, surface albedo, atmospheric absorption, scattering on molecules, clouds.

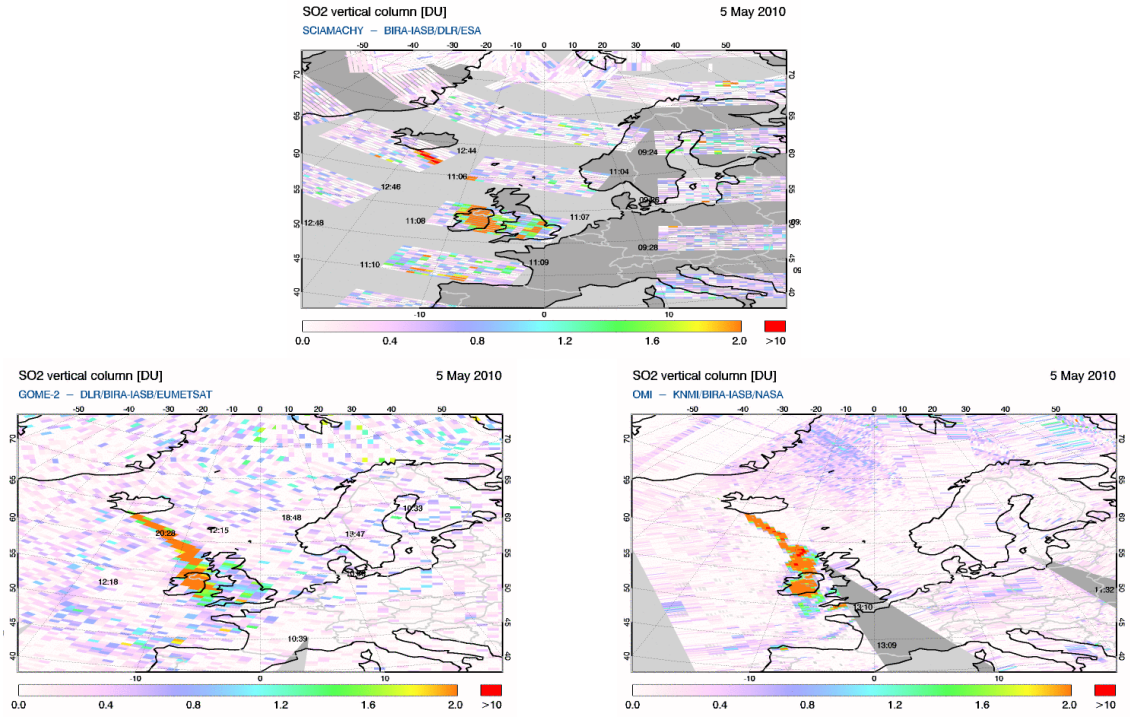

Figure 2: Examples of SO_2 vertical columns from SCIAMACHY, GOME-2 and OMI observations after the 2010 eruption of Eyjafjoll (Iceland).

Spectral fit

SCIAMACHY and GOME-2

The experience from retrievals performed using the SCIAMACHY and GOME-2 instruments (Van Geffen et al., 2007, 2008; Valks and Loyola, 2010) have led to the selection of the 315-326 nm wavelength interval, which appears as a best compromise for accurate SO_2 slant column determination using DOAS. The detection limit however depends on the observing conditions (time and place) and the solar zenith angle. In particular, the strong ozone absorption in the UV can interfere with SO_2 retrieval (see Figure 3) so that larger effective ozone absorption is a source of bias and generally results in larger background noise.

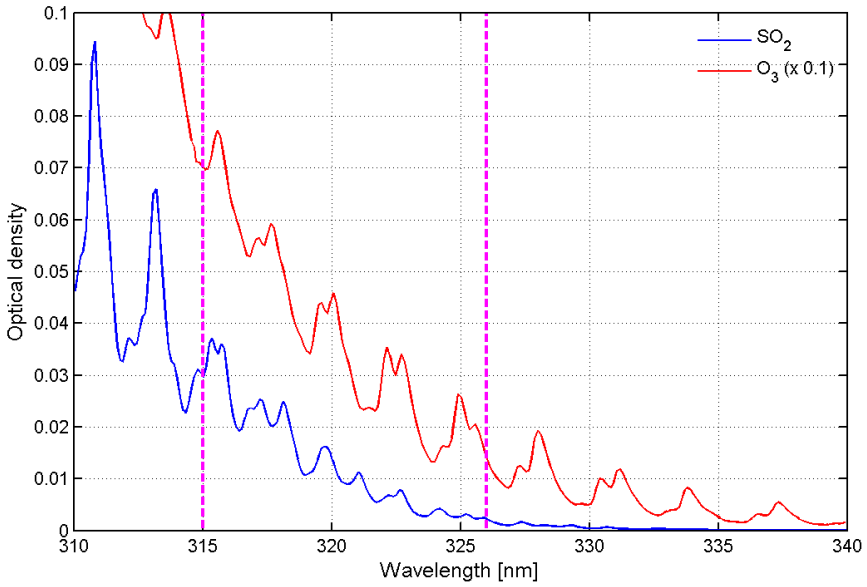

Figure 3: Typical optical densities of SO_2 and O_3 in the wavelength region from 310 to 340 nm. Note that the O_3 optical density has been divided by a factor of 10 for clarity reason.

The detailed settings for SCIAMACHY and GOME-2 SO_2 DOAS fits are summarized in Tables 1 and 2. In addition to SO_2, ozone cross-sections at two temperatures (218 and 243K are included in the fit. Furthermore two Ring spectra are fitted.

Table 1: DOAS settings used for SCIAMACHY SO_2 slant column retrieval.

Fitting interval	315 - 326 nm
Sun reference	Equatorial earthshine spectrum
Wavelength calibration	Wavelength calibration of sun reference optimized by NLLS adjustment on convolved Chance and Spurr solar lines atlas
Absorption cross-sections	
- SO_2	SCIA Flight Model [Bogumil et al., 1999], 203 K (15 km), 243 K (6 km), 273 K (2.5 km)
- Ozone	Malicet et al. [1995], 218 K and 243 K
- Ring effect	2 Ring eigenvectors generated using SCIATRAN
Polynomial	3rd order (4 parameters)
Intensity offset correction	Constant offset

Table 2: DOAS settings used for GOME-2 SO_2 slant column retrieval.

Fitting interval	315 - 326 nm
Sun reference	Sun irradiance from GOME-2 L1 product
Wavelength calibration	Wavelength calibration of sun reference optimized by NLLS adjustment on convolved Chance and Spurr solar lines atlas
Absorption cross-sections	
- SO_2	Reconvolved SCIA Flight Model [Bogumil et al., 1999], 203 K (15 km), 243 K (6 km), 273 K (2.5 km)
- NO_2	GOME-2 Flight Model/CATGAS [Gür et al., 2005], 241 K
- Ozone	Malicet et al. [1995], 218 K and 243 K
- Ring effect	2 Ring eigenvectors generated using SCIATRAN
Polynomial	3rd order (4 parameters)
Intensity offset correction	Constant offset

OMI

The TRL, TRM and STL columns are produced with the Linear Fit (LF) algorithm [Yang et al 2007]. This algorithm use a recently modified version (Version 8.5) of TOMS total ozone algorithm (OMTO3) [Bhartia and Wellemeyer 2002] as a linearization step to derive an initial estimate of total ozone assuming zero SO_2. (See OMTO3 README file for more detail). The residuals at the 10 wavelengths are then calculated as the difference between the measured and computed N-values (N=-100*log10(I/F), I is Earth radiance and F is solar irradiance) using a vector forward model radiative transfer code that accounts for multiple Rayleigh scattering, ozone absorption, Ring effect, and surface reflectivity, but assumes no aerosols. Cloudy scenes are treated as mixture of two opaque Lamberian surfaces, one at the terrain pressure and the other at Radiative Cloud Pressure (RCP) derived using OMI-measured Rotational Raman scattering at around 350 nm (see OMCLDRR README file for more detail). In the presence of SO_2, the residuals contain spectral structures that correlate with the SO_2 absorption cross-section. The residuals also have contributions from other errors sources that have not yet been identified. To reduce this interference, a median residual for a sliding group of SO_2-free and cloud-free scenes (OMTO3 radiative cloud fraction < 0.15) covering ±15° latitude along the orbit track is subtracted for each spectral band and cross-track position [Yang et al 2007]. The LF algorithm uses the corrected residuals as their inputs to derive SO_2 column amount.

SO_2 produced by volcanic degassing and eruptions can produce large errors in OMTO3 derived total ozone and can make the retrieval highly non-linear. The linear Fit (LF) algorithm was developed to handle such cases. The LF algorithm minimizes different subsets of residuals by simultaneously adjusting total SO_2, ozone and includes a

quadratic polynomial in the spectral fit. The subsets are determined by the process of dropping the shortest wavelength bands one at a time until the 322nm band is reached. The largest SO_2 retrieval is reported as the final estimate. The assumed gaseous vertical profiles correspond to the standard OMTO3 ozone profiles. The SO_2 weighting functions are approximated using OMTO3 layer Efficiency factors in Umkehr layers 0, 1 and 3, for ColumnAmountSO2_TRL, ColumnAmountSO2_TRM, and ColumnAmountSO2_STL data, correspondingly. Treatment of aerosols and clouds is the same as in the OMTO3 algorithm. (see also http://so2.umbc.edu/omi/)

Background correction

First an equatorial offset correction is applied that accounts for any systematic bias in the SO2 column. The latter correction is calculated daily/monthly (GOME-2/SCIAMACHY) based on measurements for SZA<50° (SCIAMACHY) or in a region where no sources of SO2 are present (GOME-2).
Secondly, a correction is applied to the SO_2 slant columns that accounts for the strong interference between SO_2 and ozone absorption signals in the 315-326 nm wavelength range, resulting in negative SO_2 SCDs for higher solar zenith angles. The correction depends directly on the square of the retrieved ozone slant column. The parameterization is calculated once for all for SCIAMACHY and on a yearly basis for GOME-2.

AMF calculation

For SCIAMACHY and GOME-2, the air mass factors are determined using pre-calculate look-up tables, made with an off-line radiative transfer model (LIDORT). The look-up tables have a set of entries: the viewing geometry, the solar zenith angle, the surface albedo, the cloud fraction and cloud top pressure. For OMI data the approach is rather similar, though there is no real SCD available

For the AMFs calculations, an a priori volcanic SO2 profile is assumed with a predefined central plume height. As the correct plume height is rarely available at the time of the measurement, the satellite SO_2 products provide three (GOME-2 & SCIAMACHY) or four (OMI) different vertical column densities based on the assumption about the vertical profile of the SO_2 in the atmosphere. For the three satellite instruments used here, these assumed heights are listed in Table 3.

Table 3: Assumed vertical distribution of SO_2 for satellite data sets.

Instrument	***SO_2 distribution***
GOME-2	The SO_2 is assumed to be in a 1 km thick layer centred around: • 2.5 km above sea level • 6 km above sea level • 15 km above sea level
SCIAMACHY	The SO_2 is assumed to be in a 1 km thick layer centred around: • 1 km above ground level

	• 6 km above sea level, or 1 km above ground level if that is higher • 14 km above sea level
OMI	The SO_2 is assumed to be concentrated in the: • planetary boundary layer • lower troposphere: between 0 and 5 km • middle troposphere: between 5 and 10 km • lower stratosphere: between 15 and 20 km

The lowest level for each of these cases in general represents SO_2 in the planetary boundary layer (PBL) from anthropogenic activities or passive degassing of low volcanoes. The middle tropospheric level in general represents SO_2 from effusive volcanic eruptions or passive degassing of high volcanoes. The lower stratospheric level represents SO_2 from explosive volcanic eruptions.

3.2 SO2 plume height retrieval from UV-visible observations: GOME-2

The SO_2 fitting window in the UV not only contains information on the total vertical SO_2 column amount, but to certain extend also on the height of the SO_2 gas. The way the SO_2 concentration at different altitudes in the atmosphere is sampled by the satellite measurements is wavelength dependent and is strongly influenced by the altitude profile of ozone. It can be shown (Yang *et al.*, 2010) that the weighting functions of the measured reflectance spectrum with respect to the total vertical SO_2 column and SO_2 height can respectively be expressed as:

$$W_N = \frac{\partial \ln I_{\mathrm{TOA}}}{\partial N} - \sigma \cdot m \qquad (1)$$

and

$$W_z = \frac{\partial \ln I_{\mathrm{TOA}}}{\partial z} = -N \cdot \sigma \cdot \frac{\partial m}{\partial z} \qquad (2)$$

Here we assume an SO_2 amount of total column N, confined to an infinitesimally thin layer at altitude z. I_{TOA} is the measured spectrum at top-of-atmosphere. Through the absorption cross section σ, the wavelength dependence of both weigthing functions would appear very similar, particularly for narrow fitting-windows. However, the weighting functions are modulated by the SO_2 air-mass factor m and its derivative, respectively (Figure), though which the shape of these weighting functions appear different. In other words, changing the total column amount has a different effect on the measured spectrum than a change of altitude of an SO_2 plume of fixed total column, thus providing us with the possibility to derive height information from the measurements.

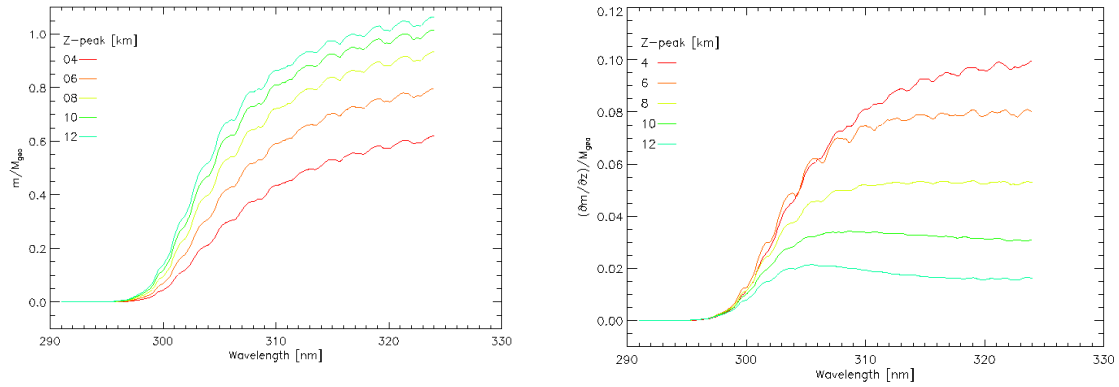

Figure 4: Wavelength dependency of the air-mass factor (AMF) m (left) and its derivative with respect to altitude, for a selected range of SO_2 plume altitudes. The curves are normalized with the geometrical AMF, Mgeo. The shape difference between these two types of profile provides information on the altitude of the plume in satellite measurements.

When deriving an altitude of the SO_2 plume through a direct fitting algorithm, the plume has to be represented in the model atmosphere. Here we have chosen to parametrize volcanic plumes by means of a general distribution function, which provides a simple mathematical description of a distinctively peaked plume and has an analytical derivative. The initial parametrized plume is defined by a top and bottom height, peak height, and a half width value.
The peak altitude resulting from the retrieval precess is an effective height. This means that any effects of aersosol (which are not treated explicitly), inhomogeneities of the horizontal SO_2 distribution or deviation from the parametrized plume shape are incorporated in the result.

3.3 SO2 index retrieval from infrared observations: IASI

The SO_2 molecule has several strong absorption features in the infrared that are covered by the IASI instrument. The strongest of the bands is the ν_3 band centre at 1362 cm^{-1}. The ν_1 band centre at 1152 cm^{-1} is also observed but is weaker. The detection of SO_2 by IASI is that of an index, i.e. it is given by the change in brightness temperature (expressed in Kelvin) in the selected channels due to a loading of SO_2. The advantage of this approach is that it is computationally very fast, and it enables to identify and track volcanic plumes well, thanks to the high spatial and temporal sampling and good radiometric performances of IASI (Clarisse et al., 2008). The noise equivalent delta temperature is estimated to be of 0.05 K in the ν_3 band and 0.12 K in the ν_1 band. The absorption channels were chosen to maximize the sensitivity above 3 km. Below this altitude, the measurement sensitivity almost vanishes in the ν_3 band. Nonetheless, IASI is theoretically capable of sensing SO_2 in the boundary layer using the ν_1 band, but it will depend strongly on the local atmospheric conditions in terms of SO_2 content, water vapour profile and the thermal contrast between the surface and the boundary layer. Note that beyond the simple SO_2 index approach, concentrations and vertical profiles of SO_2 can be retrieved using a sophisticated line-by-line radiative transfer model and an

inverse off-line code using the optimal estimation method (see details in Clarisse et al., 2008).

For SACS+ an alternative retrieval method has been designed, which relies solely on the SO2 index and an assumed plume altitude. The approach starts with calculating the IASI SO_2 index as the difference in brightness temperature of the baseline channels at 1407.25 and 1408.75 cm^{-1} (referred to as T_B); and the ν_3 channels at 1371.50 cm^{-1} and 1371.75 cm^{-1} (referred to as $T_{\nu 3}$). The temperature of atmospheric layer which contains the SO2 plume will be denoted T_{SO2}. These different temperatures are illustrated in Figure 5.

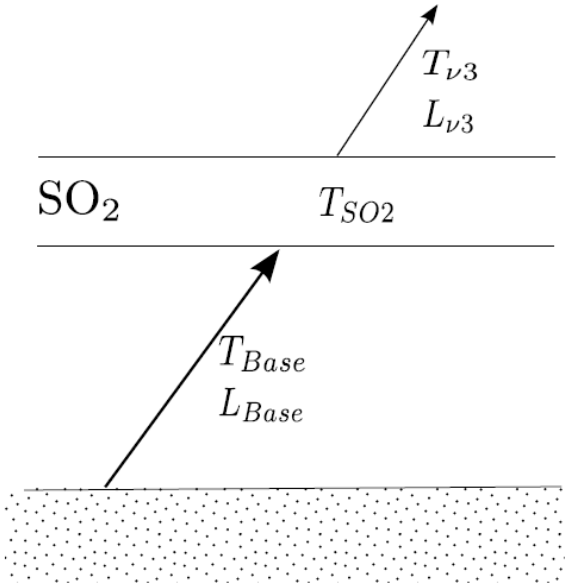

Figure 5: Schematic view of the different temperatures used in the retrieval. As T_B and T_{v3} can be calculated directly from the spectrum; T_{SO2} is assumed.

Using elementary radiative transfer, it can be shown that the SO2 partial column C can be approximated by

$$C = -\frac{\cos\theta}{c_1} \ln\left(\frac{(\exp(A/T_{\mathrm{B}}) - 1)(\exp(A/T_{\mathrm{SO2}}) - \exp(A/T_{\nu 3}))}{(\exp(A/T_{\nu 3}) - 1)(\exp(A/T_{\mathrm{SO2}}) - \exp(A/T_{\mathrm{B}}))}\right). \quad (3)$$

with Θ the satellite viewing angle, and c_1 is a coefficient which depends on temperature, pressure and the specific sounder (e.g. the spectral response function and spectral sampling). For SACS+ these coefficients have been assumed to depend on altitude only, and subsequently which mean precalculated values are used for 8 different altitudes (5,7,10,13,16,19,25,30). Errors are also estimated and vary from 30% for the lowest and highest altitudes to 5% in the tropopause. The formula also allows to put elementary constraints in altitude in case of high loadings. Namely, T_{SO2} can never be higher than T_{v3} puts a lower bound on T_{SO2}. If this is the case, the argument of the logarithm in the equation above becomes negative. An example of the retrieval and impossible altitudes

are illustrated in the figure below, in which case we can deduce a lower bound of 10km on the plume altitude.

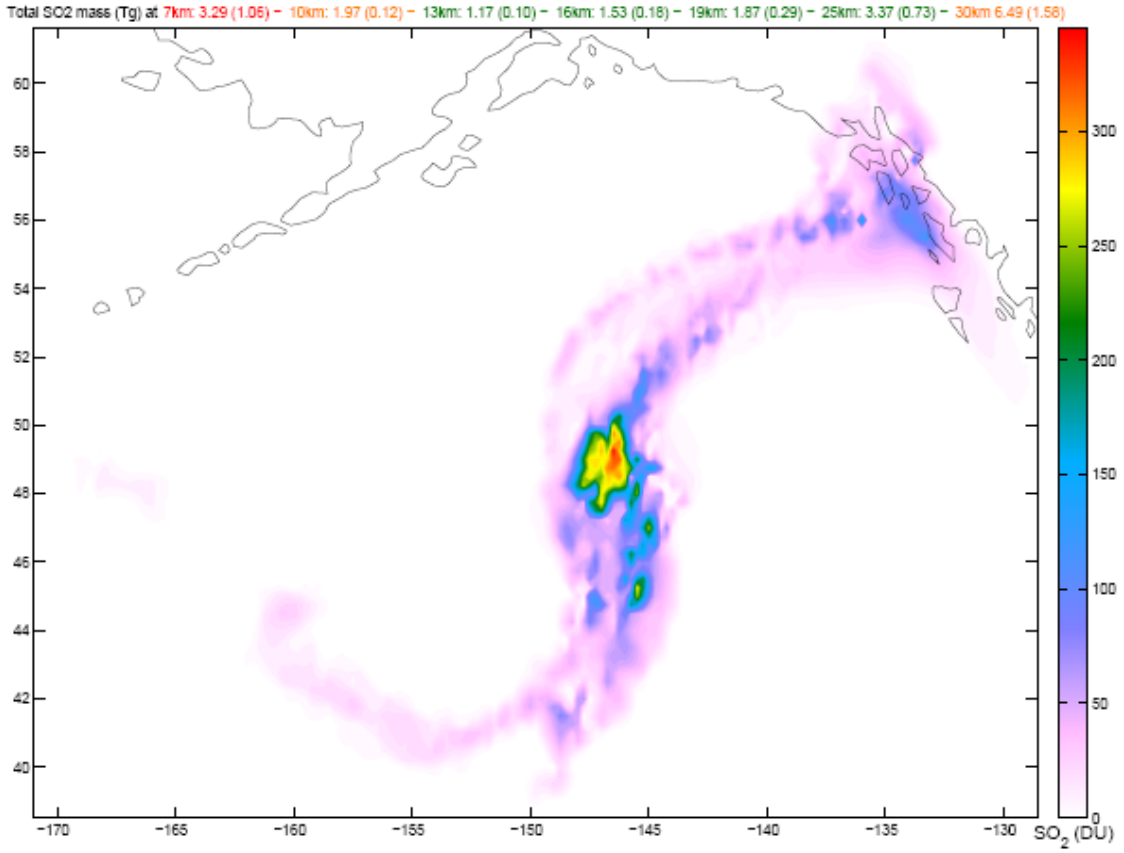

Figure 6: An SO2 plume retrieval after the 2008 Kasatochi eruption, assuming 7 different plume altitudes. Altitudes in red and orange correspond to respectively 50% and 10% pixels for which the altitude is physically impossible.

4 Aerosols algorithms

4.1 Absorbing aerosol index retrieval from UV-visible observations: SCIAMACHY, OMI and GOME-2

The Absorbing Aerosol Index (AAI) is an indicator for the presence of elevated absorbing aerosols in the atmosphere. It is a widely used product as it is rather simple to implement in an operational environment (Hermann et al., 1997, Tilstra et al., 2007). The calculation of AAI is based on a residual that separates the spectral contrast at two ultraviolet wavelengths caused by absorbing aerosols from that of other effects, including molecular Rayleigh scattering, surface reflection, gaseous absorption and aerosol and cloud scattering. The AAI product is not strictly selective for volcanic ash, as important aerosol types are also UV-absorbing: desert dust aerosols and biomass burning aerosols. However, the AAI has already be shown to be useful in tracking plumes when the SO2 signal is not detectable (this was precisely the case for the Eyjafjoll eruption). Furthermore, the combined detection of both elevated AAI and SO_2 is highly selective for the volcanic plume (in fact even more than SO_2 detection alone) and therefore it helps to better assess the location and coverage of the volcanic plume (see Figure 7).

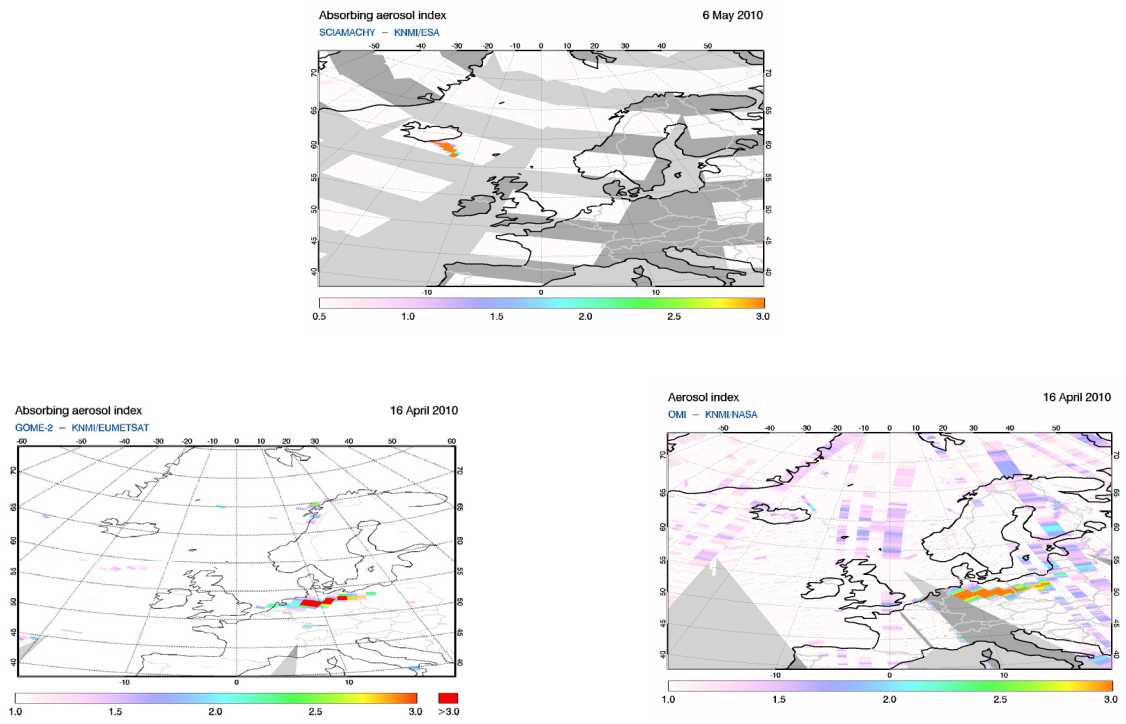

Figure 7: Examples of Absorbing Aerosol Indexes from SCIAMACHY, GOME-2 and OMI observations after the 2010 eruption of Eyjafjoll (Iceland).

The absorbing aerosol index is a wavelength-dependent variable defined as:

$$AI_\lambda = -100 \cdot \left\{ \log_{10}\left(I_\lambda / I_{\lambda 0}\right)^{meas} - \log_{10}\left(I_\lambda / I_{\lambda 0}\right)^{Ray} \right\} \quad (4)$$

where I_λ is the radiance at the top of the atmosphere (TOA) at a wavelength λ. I^{meas} refers to a measured TOA radiance of a real atmosphere with aerosols, as opposed to a calculated TOA radiance for an aerosol-free atmosphere with only Rayleigh scattering and absorption by molecules and surface reflection and absorption (I^{Ray}).
Let us defined the reflectance as:

$$R = \frac{\pi I}{\mu_0 E_0} \quad (5)$$

where E_0 is the solar irradiance at TOA and μ_0 is the cosine of the solar zenith angle. We can rewrite equation 4 in terms of reflectance. If the surface albedo A_s for the Rayleigh atmosphere calculation is chosen so that:

$$R_{\lambda 0}^{meas} = R_{\lambda 0}^{Ray}(A_s) \quad (6)$$

where λ_0 is a reference wavelength. Equation (4) becomes:

$$AI_\lambda = -100 \cdot \log_{10}\left[\frac{R_\lambda^{meas}}{R_\lambda^{Ray}}\right] \quad (7)$$

where R_λ^{Ray} is calculated for surface albedo $A_s(\lambda_0)$, so the surface albedo is assumed to be constant in the range $[\lambda, \lambda_0]$. It should be stressed that when a positive residue is found, absorbing aerosols are detected. Negative or zero residues on the other hand, suggest an absence of absorbing aerosols.

The calculation of AAI (equation 7) involves:
- finding a surface albedo for which the measured reflectance at the reference wavelength is equal to the reflectance of a pure Rayleigh atmosphere with all scattering and absorption effects accounted for in the surface albedo. This inversion process is usually performed with lookup tables of the reflectances, generated off-line with an appropriate radiative transfer model.
- a correct absolute calibration of the reflectance for obtaining reliable AAI data.

The wavelength pair 340 and 380 nm are measured in different channels of the OMI instrument; 340 nm is in the UV channel and 380 nm in the VIS channel of the instrument. Therefore, for the AAI calculation of OMI a different wavelength pair, shown in Table 4. is chosen, which is measured in a single channel.

Table 4: Wavelengths pair used for the calculation of AAI for different satellite UV-visible instruments.

Instrument	***Wavelengths pair***
SCIAMACHY	340 and 380 nm
OMI	354 and 388 nm
GOME-2	340 and 380 nm

The algorithm is using look-up tables (LUTs) to find the theoretical calculated scattered radiances for the wavelength pairs. The LUTs were created using the radiative transfer code DAK (which stands for "Doubling-Adding KNMI", De Haan et al. 1987). This vector RTM takes polarisation into account, as well as ozone absorption and Lambertian surface reflection. A pseudo-spherical version of the RTM DAK was used. Also, O2–O2 absorption is included in the radiative transfer calculations of the LUTs. A fixed O2 background concentration is used, which is a justified simplification. The different parameters for the LUT are surface albedo, relative azimuth angles, zenith angles, ozone column values (50, 200, 300, 350, 400, 500, 650 DU), and surface heights (ranging from 0 to 8 km in 1 km steps).

4.2 Ash index retrieval from infrared observations: IASI

The ash index, is like the SO_2 index based on the difference in temperature between two channels, namely at 1231.5 and 1168 cm^{-1}. As illustrated in the figure below, this difference is very sensitive for all types of ash, but may also flag on other mineral dust. For this reason, this index is only indicative for ash in case of simultaneous detection of SO_2. Even then, caution will need to be exerted in the interpretation of this index as both SO_2 and other mineral dust can yield contamination.

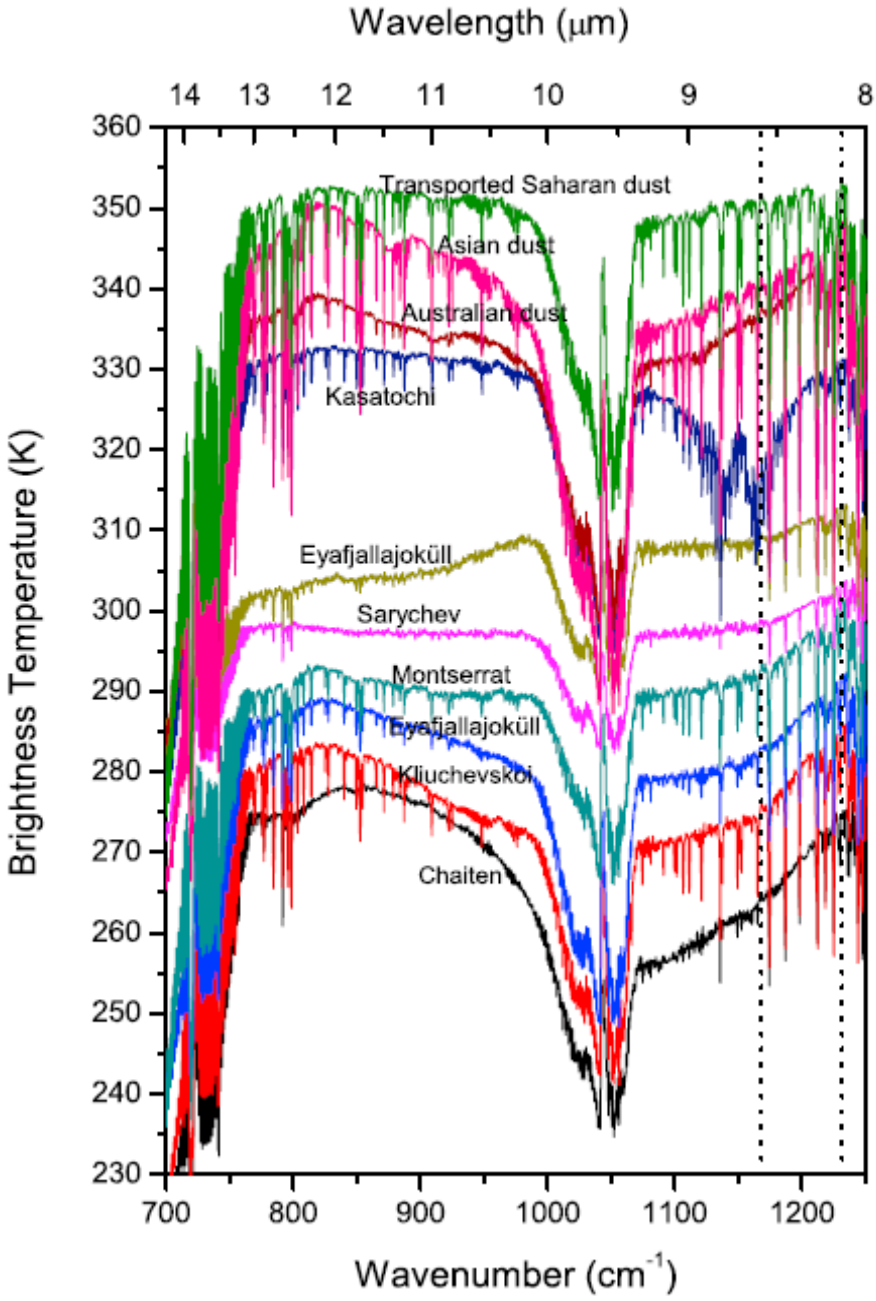

Figure 8: IASI observations of 3 dust storms and 7 volcanic ash plumes The dotted lines show the location of the reference channels for the calculation of the ash brightness temperature difference (see Clarisse 2010).

5 References

Bhartia, P. K. and C. W. Wellemeyer, OMI TOMS-V8 Total O3 Algorithm, Algorithm Theoretical Baseline Document: OMI Ozone Products, edited by P. K. Bhartia, vol. II, ATBD-OMI-02, version 2.0., 2002. Available: http://eospso.gsfc.nasa.gov/eos_homepage/for_scientists/atbd/docs/OMI/ATBD-OMI-02.pdf.

Bovensmann, H., Burrows, J.P., Buchwitz, M., Frerick, J., Noël, S., Rozanov, V.V., Chance, K.V., Goede, A.P.H., SCIAMACHY: Mission objectives and Measurement Modes, J. Atm. Sci., 56, 127-150, 1999.

Clarisse, L., Coheur, P.-F., Prata, A.J., Hurtmans, D., Razavi, A., Phulpin T., Hadji-Lazaro, J., and Clerbaux, C.: Tracking and quantifying volcanic SO_2 with IASI, the September 2007 eruption at Jebel at Tair, Atmos. Chem. Phys., 8, 7723-7734, 2008.

Clarisse, L., Prata, F., Lacour, J.-L., Hurtmans, D., Clerbaux, C., and Coheur, P.F. : A correlation method for volcanic ash detection using hyperspectral infrared measurements, Geophys. Res. Lett., 37, L19806, doi:10.1029/2010GL044828, 2010.

Clerbaux, C., Boynard, A., Clarisse, L, George, M., Hadji-Lazaro, J., Herbin, H., Hurtmans, D., Pommier, M., Razavi, A., Turquety, S., Wespes, C., and Coheur, P.-F.: Monitoring of atmospheric composition using the thermal infrared IASI/MetOp sounder, Atmos. Chem. Phys., 9, 6041-6054, 2009.

de Haan, J. F., P. B. Bosma, and J. W. Hovenier, The adding method for multiple scattering calculations of polarised light, Astron. Astrophys., 183, 371–391, 1987.

Herman, J. R., P. K. Bhartia, O. Torres, C. Hsu, C. Seftor, and E. Celarier, Global distributions of UV-absorbing aerosols from Nimbus 7/TOMS data, J. Geophys. Res., 102(D14), 16,911–16,922, doi:10.1029/96JD03680, 1997.

Levelt, P.F., van den Oord, G.H.J., Dobber, M.R., Mälkki, A., Visser, H., de Vries, J., Stammes, P., Lundell, J.O.V., and Saari, H.: The Ozone Monitoring Instrument, IEEE Trans. on Geosci. Rem. Sens., 44(5), doi:10.1109/TGRS.2006.872333,2006a.

Munro, R., Eisinger, M., Anderson, C., Callies, J., Corpaccioli, E., Lang, R., Lefebvre, A., Livschitz, Y., and Albinana, A. P.: GOME-2 on MetOp, in: Proc. of The 2006 EUMETSAT Meteorological Satellite Conference, Helsinki, Finland, 12–16 June 2006, EUMETSAT P.48, 2006.

L.G. Tilstra, M. de Graaf, I. Aben, and P. Stammes, Analysis of 5 years of SCIAMACHY Absorbing Aerosol Index data, Proceedings of the 2007 Envisat Symposium, ESA Special Publication SP-636, 2007.

Valks, P., and Loyola, D., Algorithm Theoretical Basis Document for GOME-2 Total Column Products of Ozone, Minor Trace Gases and Cloud Properties (GDP 4.4 for O3MSAF OTO and NTO), O3MSAF, DLR/GOME-2/ATBD/01, 2010.

Van Geffen, J., Van Roozendael, M., Di Nicolantonio, W., Tampellini, L., Valks, P., Erbetseder, T. and Van der A, R.: Monitoring of volcanic activity from satellite as part of GSE PROMOTE, in Proceedings of the 2007 ENVISAT Symposium, 23-27 April 2007, Montreux, Switzerland, ESA publication SP-636, 2007.

Van Geffen, J., Van Roozendael, M., Rix, M., Valks, P.: Initial validation of GOME-2 GDP 4.2 SO_2 total columns (OTO/SO2) – ORR B, O3MSAF validation report, TN-IASB-GOME2-O3MSAF-SO2-01.1, 2008.

Yang, K., N. Krotkov, A. Krueger, S. Carn, P. K. Bhartia, and P. Levelt, Retrieval of Large Volcanic SO2 columns from the Aura Ozone Monitoring Instrument (OMI): Comparisons and Limitations, J. Geophys. Res., 112, D24S43, doi:10.1029/2007JD008825, 2007.

Yang, K., Liu, X., Bhartia, P., Krotkov, N., Carn, S., Hughes, E., Krueger, A., Spurr, R., Trahan, S.: Direct retrieval of sulfur dioxide amount and altitude from spaceborne hyperspectral UV measurements: Theory and application, J. Geophys. Res., 115, D00L09, doi:10.1029/2010JD013982, 2010.